AFOSR-TR-97-0454

REPORT DOCUMENTATION PAGE

Form Approved
OMB No. 0704-0188

1. AGENCY USE ONLY (Leave blank)	2. REPORT DATE	3. REPORT TYPE AND DATES COVERED
	31 July 1997	Final Report 15 May 93 - 14 May 97

4. TITLE AND SUBTITLE
Coaxial Vircator, High-Power Microwave Development

5. FUNDING NUMBERS
61102F
2301/ES

6. AUTHOR(S)
M. Kristiansen, L. L. Hatfield, Kevin Woolverton

7. PERFORMING ORGANIZATION NAME(S) AND ADDRESS(ES)
Pulsed Power Laboratory
Texas Tech University, MS-3102
Lubbock, TX 79409-3102

8. PERFORMING ORGANIZATION REPORT NUMBER

9. SPONSORING/MONITORING AGENCY NAME(S) AND ADDRESS(ES)
AFOSR/NE
110 Duncan Ave, Suite B115
Bolling AFB, DC 20332-001

10. SPONSORING/MONITORING AGENCY REPORT NUMBER
F49620-93-1-0203

11. SUPPLEMENTARY NOTES

12a. DISTRIBUTION/AVAILABILITY STATEMENT
APPROVED FOR PUBLIC RELEASE: DISTRIBUTION UNLIMITED

12b. DISTRIBUTION CODE

13. ABSTRACT *(Maximum 200 words)*

The purpose for this contract was to build , test and study the coaxial vircator. This work is the continuation of AFOSR Grant No. F49620-93-10203. A study of the efficiency of a coaxial virtual cathode oscillator is presented. The coaxial geometry has many physical parameters that can be changed to alter performance. These parameters include the placement of an annulus cut in the anode base, the polarity of the system, and the variation of the applied voltage. The annulus creates a decelerating field for the electrons and tends to keep them in the right-phased region of the virtual cathode. The annulus is varied in width and in position from the center line with the results normalized to the no annulus geometry. The results for a positively and negatively pulsed system, and the results of changing the applied voltage are also given. Comparisons of frequency, efficiency, and particle dynamics of the positively and negatively pulsed systems are given. MAGIC, a 2-1/2 dimensional particle-in-cell code, and SOS, a 3 dimensional particle-in-cell code, are used to simulate the different geometries.

14. SUBJECT TERMS	15. NUMBER OF PAGES
Microwaves, Radio Frequency	31
	16. PRICE CODE

17. SECURITY CLASSIFICATION OF REPORT	18. SECURITY CLASSIFICATION OF THIS PAGE	19. SECURITY CLASSIFICATION OF ABSTRACT	20. LIMITATION OF ABSTRACT
UNCLASSIFIED	UNCLASSIFIED	UNCLASSIFIED	NONE

NSN 7540-01-280-5500

Standard Form 298 (Rev. 2-89)
Prescribed by ANSI Std. 239-18
298-102

Final Technical Report
On

HIGH POWER MICROWAVE GENERATOR

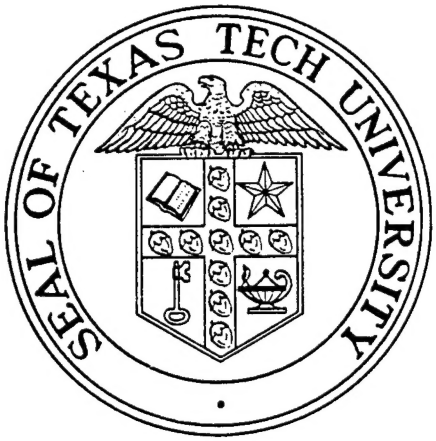

July 31, 1997

Air Force Office of Scientific Research

Grant No. F49620-93-1-0203

PULSED POWER LABORATORY
DEPARTMENT OF ELECTRICAL ENGINEERING
TEXAS TECH UNIVERSITY
LUBBOCK, TEXAS 79409-3102

Executive Summary

This is the final technical report for AFOSR Grant No. F49620-1-0203 which began on May 15, 1993. The goal of this contract period was to study the mechanisms of the coaxial vircators to be able to increase the efficiency. This work is the continuation of efforts which were begun under AFOSR Grant No. 91-0260. This report covers the design of the coaxial vircator and the simulations and results of changing the original design geometry. The changes include adding a collection rod down the center, a hole down the center, or an annulus in the anode base. Other changes include changing the polarity on the diode and varying the charging voltage.

The particle-in-cell simulation codes MAGIC and SOS have been used to simulate the geometries. Voltage, current, impedance, efficiency, frequency and power characteristics have been obtained from the simulations. Animations of the simulations have been created and used to gain a better insight into the working mechanisms of the coaxial vircator. The animations created show particle motion in the vircator at various positions inside the vircator and phase-space plots in the radial and axial directions.

This report discusses the results from the study of the coaxial vircator. Mechanisms of operation and efficiency improvements will be discussed. It was found that placing a rod down the center decreased the efficiency by drawing more electrons into the wrong-phased region, the region where energy is given to accelerating electrons instead of the electrons slowing down and giving up their energy to microwave energy. Placing a hole in the center increased the efficiency by keeping the electrons in the right-phased region. An annular indentation could also be used to further increase the efficiency. Pulsing the geometry negatively gave a mechanism for electrons to be

expelled out of the interaction region resulting in an increase in efficiency. Finally, the applied voltage is important in the coaxial vircator geometry, it allows the plasma and reflexing frequency of the virtual cathode to be matched, resulting in a higher efficiency.

Many factors have been found to be important in increasing the output power and efficiency of the coaxial vircator. The most important being a loss mechanism for electrons which allows new electrons to enter the virtual cathode region and generate microwaves. A negative polarity system provides this kind of mechanism. The interaction of electrons in the interaction region is also important. Keeping electrons in the right-phased region and out of the wrong-phased region can keep the efficiency high. The placement of an annulus in the anode base at the appropriate width and distance from the center line creates a field that keeps electrons in the right-phase region and the efficiency high. Finally, the applied voltage level can be adjusted to match the reflexing and plasma frequencies, resulting in an increase in efficiency.

Principal Investigators: Dr. M. Kristiansen, C. B. Thorton/P. W. Horn Professor of Electrical Engineering and Physics
Dr. L. L. Hatfield, Professor of Physics

Graduate Students: Mark Crawford,
Kevin Woolverton

Publications:

1. "Computer Simulations of Coaxial Vircators", SPIE's 42nd Annual Meeting, San Diego, CA, July 27 – August 1, 1997, K. Woolverton, M. Kristiansen, L. L. Hatfield.

2. "Diode Polarity Experiments On A Coaxial Vircator", 24th Int'l. Conf. On Plasma Science, San Diego, CA, May 19-22, 1997, K. Woolverton, M. Kristiansen, L. L. Hatfield.

3. "A Study of Coaxial Vircator Geometries" Research and Development Summer Research Publication at Phillips Lab, NM, August, 1996, K. Woolverton.

4. "Coaxial Vircator Source Development", 11th Int'l. Conf. On High Power Particle Beams, Prague, Czech Republic, June 10-14, 1996, K. Woolverton, M. Kristiansen, L. L. Hatfield.

5. "Experimental Results from a Coaxial Virtual Cathode Oscillator", 10th IEEE International Pulsed Power Conference, Albuquerque, NM, July 10-13, 1995, M. Crawford, M. Kristiansen, L. L. Hatfield.

6. "Results from a Coaxial Vircator: Experiment and Simulation", 7th National Conference on High Power Microwave Technology, Oct. 31 - Nov. 4, 1994, Monterey, CA, M. Crawford, M. Kristiansen.

7. "Comparison Between Simulation and Experiment on a Coaxial Vircator High-Power Microwave System", 10th International Conference on High Power Particle Beams, June 20-24, 1994, San Diego, CA, M. Crawford, M. Kristiansen.

8. "Cylindrically-Symmetric Virtual Cathode Oscillator High-Power Microwave Source", 9th IEEE Pulsed Power Conference, Albuquerque, NM, June 21-23, 1993, M. Crawford, M. Kristiansen, L. L. Hatfield.

9. "Computer Assisted Diagnostics on a High-Power Microwave System", 9th International Conference on High Power Particle Beams, Washington, DC, May 25-29, 1992, M. Crawford, M. Kristiansen, Steve Calico, L. L. Hatfield.

10. "Pulsed Microwave Breakdown of Solid Dielectric/Gas Interfaces", International Conference on Phenomena in Ionized Gases, Pisa, Italy, July 8-12, 1991, M. Crawford, M. Kristiansen, Steve Calico, L. L. Hatfield.

11. "Pulsed Vacuum Diode Diagnostics at the Texas Tech University High Power Microwave Facility", 8th Pulsed Power Conference, San Diego, CA, June 17-19, 1991, M. Crawford, M. Kristiansen, Steve Calico.

12. "The Design and Calibration of a Very Fast Current Probe for Short Pulse Measurements", Rev. of Scientific Instruments, 62, 1511 (1991), Steve Calico, M. Kristiansen, M. Crawford, H. Krompholz.

13. "Electrical Diagnostics on a High-Power Microwave Generator", MSEE at Texas Tech University, Mark Crawford, August 1991.

14. "A Coaxial Virtual Cathode Oscillator High-Power Microwave Source", Ph.D. at Texas Tech University, Mark Crawford, December 1994.

Introduction

Vircators are high-power microwave sources based on the bremsstrahlung radiation of relativistic electrons oscillating in electrostatic fields and are important microwave sources due to their simplicity and the fact that no external magnetic field is required for their operation. They require no heavy external coils with high-current power supplies. Vircators have also been shown to be tunable over a range of about two octaves and able to be phase locked. They are also capable of producing pulses on the order of a microsecond. Yet, vircators are not very efficient with typical efficiencies on the order of 2% for vircators with axial extraction and 0.6% for vircators with transverse extraction[1]. Hence, improvement in efficiency is an important area. Many geometries have been studied to increase efficiency, including the reflex triode, the reditron and more recently the virtode[2].

The virtual cathode is formed by exceeding the space charge limiting current, resulting in a depressed electrostatic field which overcomes the kinetic energy of incoming electrons. The electrons decelerate giving up energy to the microwave field. Then the electrons are accelerated away from the virtual cathode back toward the anode and toward the real cathode in a process called reflexing. This reflexing continues and produces microwaves at a frequency proportional to the square root of the applied potential and inversely proportional to the anode-cathode gap spacing. But this is not the only mechanism for microwave production. When the virtual cathode forms, it is highly unstable and it changes in magnitude and position which is another mechanism for microwave production. This occurs at the plasma frequency of the virtual cathode.

In a planar geometry when the virtual cathode magnitude is large, electrons accelerated toward the virtual cathode get repelled and oscillate in the region near the anode. This starves the virtual cathode and it decreases in magnitude. When the virtual cathode magnitude is lower, fewer electrons are repelled allowing the electron beam to propagate, hence bunches of electrons will propagate away from the virtual cathode. The virtual cathode itself is a store of the beam's kinetic energy and since bunches of electrons are lost every cycle of the virtual cathode, it has a low efficiency. If these electrons could be recovered, efficiency could be improved. The coaxial vircator on the other hand provides a built-in mechanism for electron recovery which could increase the efficiency.

Project Overview

The development of the coaxial vircator was designed around the existing pulsed power system which had been previously used to power a planar vircator for vacuum/atmosphere interface breakdown studies. The existing equipment consisted of a 10 Ω pulse-forming line (PFL) with a one-way transit time of 12.5 ns, giving a pulse length of 25 ns into a matched load, charged by a 31 stage Marx generator capable of generating 1.5 MV which is switched into the vacuum diode by a self-breaking oil spark gap. Both the Marx gererator and the PFL are insulated with transformer oil, and there is a pumping and storage system which provides a way to handle the 2800 gallons of Univolt 61 needed to fill the Marx tank and PFL. The vacuum chamber is evacuated by two mechanical roughing pumps and one 8" diffusion pump. The end of the waveguide is contained in an electrically-sealed anechoic chamber. Figure 1 shows the layout of the pulsed power system.

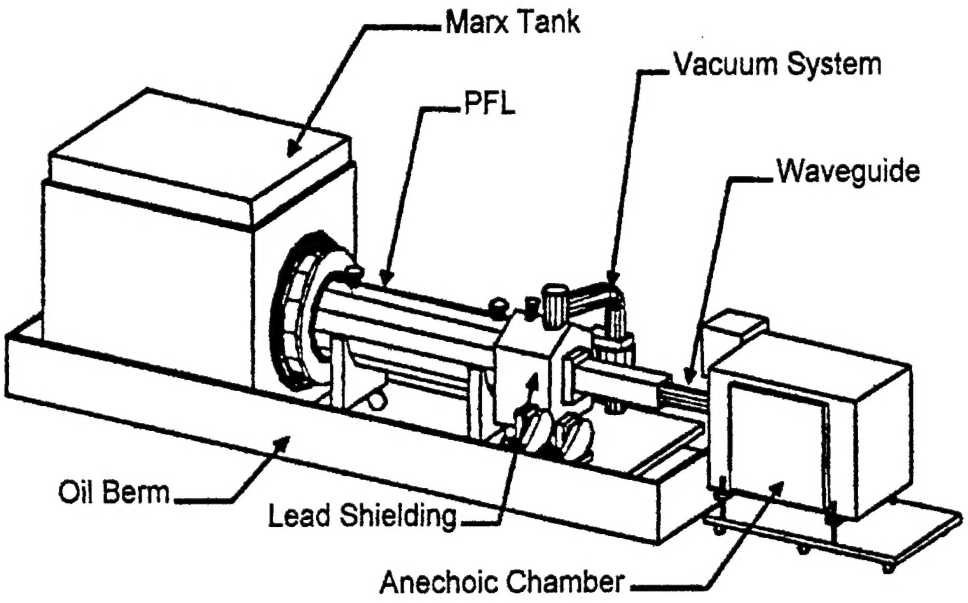

Figure 1: Schematic layout of equipment.

Coaxial Vircator Design

The coaxial vircator is based on the same principles as the planar vircator. It is based on an idea originally published by Grigoryev[3]. Instead of placing a planar cathode a short distance from a planar anode, a cylindrical cathode is placed around a cylindrical anode. Figure 2 shows a three-dimensional cut-away sketch of a coaxial vircator. The inner conductor is pulsed to a positive potential with respect to the outer conductor. Electrons are accelerated towards the center of the geometry. As the electrons pass through the anode, they slow down and stop, forming a toroidal virtual cathode. Because the electrons form the virtual cathode from all directions, it is believed that the

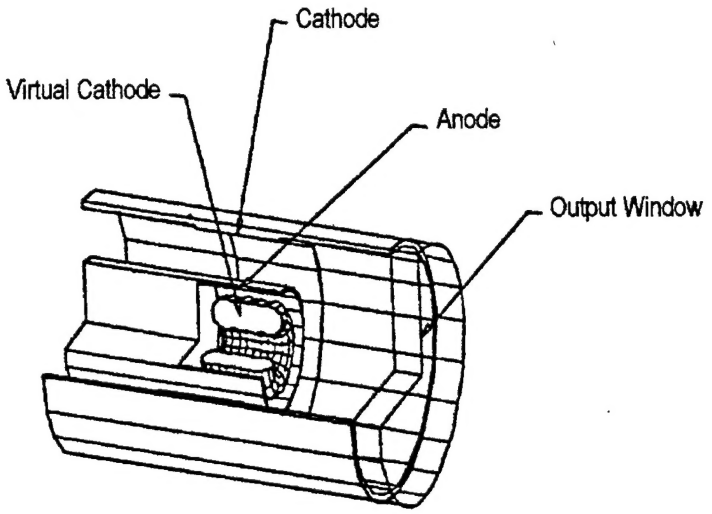

Figure 2: Cut-away schematic of the coaxial vircator

virtual cathode will be more dense and increase the efficiency of the microwave generation. This geometry lends itself to connecting directly to an output waveguide.

Previous MAGIC simulations used in designing the coaxial vircator set various vircator geometry parameters and left others variable. Table 1 shows these geometry parameters. Figures 3 and 4 below show the coaxial vircator system and cut-away view of the vircator diode respectively.

Table 1: List of design parameter values for the coaxial vircator.

Parameter	Description	**Value**
r_{gw}	Waveguide radius	98.4 mm
r_a	Anode radius	98.4 mm
r_k	Cathode radius	131.7 mm
l_a	Anode length	variable
l_k	Cathode length	variable
transition	Type of cathode-waveguide transition	45 degree angle
l_{at}	Distance between anode and transition	variable
l_{kt}	Distance between cathode and transition	variable

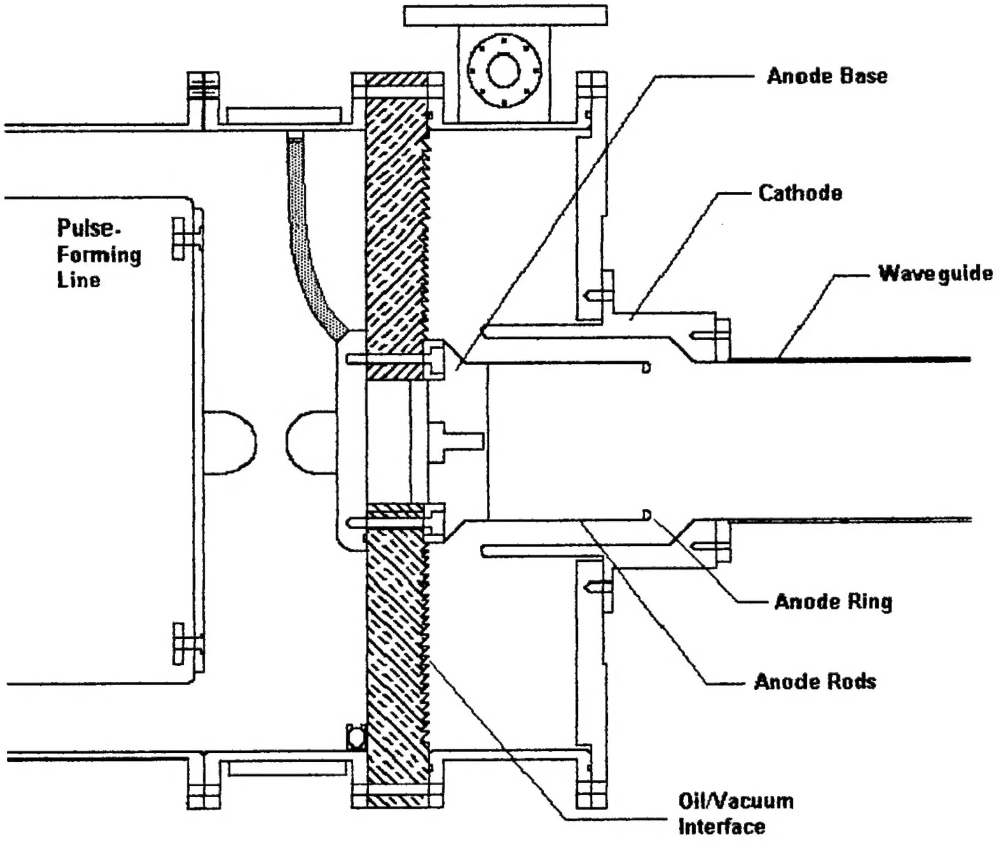

Figure 3: Coaxial vircator installed in the pulsed power system.

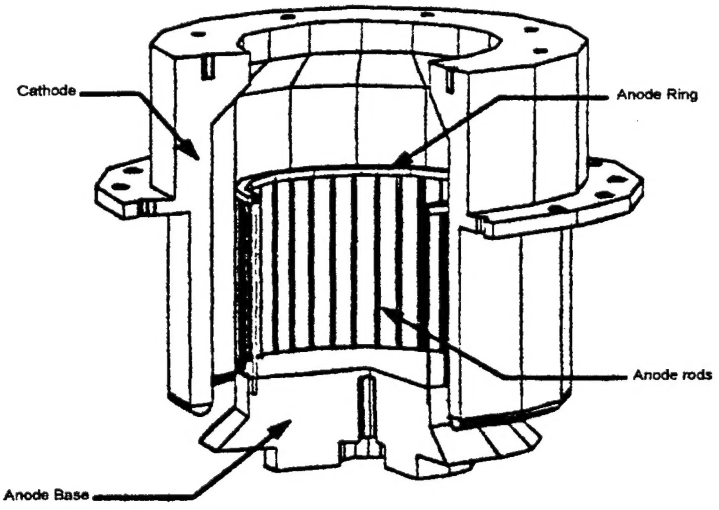

Figure 4: Cut-away view of the coaxial vircator diode.

Initial MAGIC Simulations

When testing of the vircator began, it was found that extending the cathode beyond the anode reduced the number of breakdowns. Also, the only parameters that can be varied, short of building an entirely new anode-cathode structure, are the length and axial position of the anode and cathode. This gave rise to three models to be simulated using MAGIC: a model where the anode and cathode use the entire length of the cathode structure (Model A), one with a shorter anode and cathode placed away from the cathode-waveguide transition (Model B), and one with a short anode and cathode placed near the transition (Model C). Table 2 shows the model parameters.

Table 2: Variable parameters for MAGIC simulation.

Geometry	l_a **anode length**	l_k **cathode length**	l_{at} **anode position**	l_{kt} **cathode position**
Model A	186.5 mm	208.7 mm	35.5 mm	6.7 mm
Model B	93.2 mm	208.7 mm	128.8 mm	6.7 mm
Model C	93.2 mm	93.2 mm	44.4 mm	44.4 mm

The results[4] from the MAGIC simulations are contained in tables 3-5 and figures 5-7.

Initial Experimental Results

As seen in the cut-away view of the anode structure, metal rods were the only forming structure of the anode across from the cathode and, when tested, gave results much lower than the simulation. Initially, it was thought that the rods were not conductive enough and were sent off to be silver plated. Meanwhile, the rods of Model C were wrapped with a stainless steel mesh and tested. This improved the microwave power dramatically.

The improved power became large enough to excite radiation patterns in a panel of neon bulbs well enough to see what mode was propagated. An unexpected result

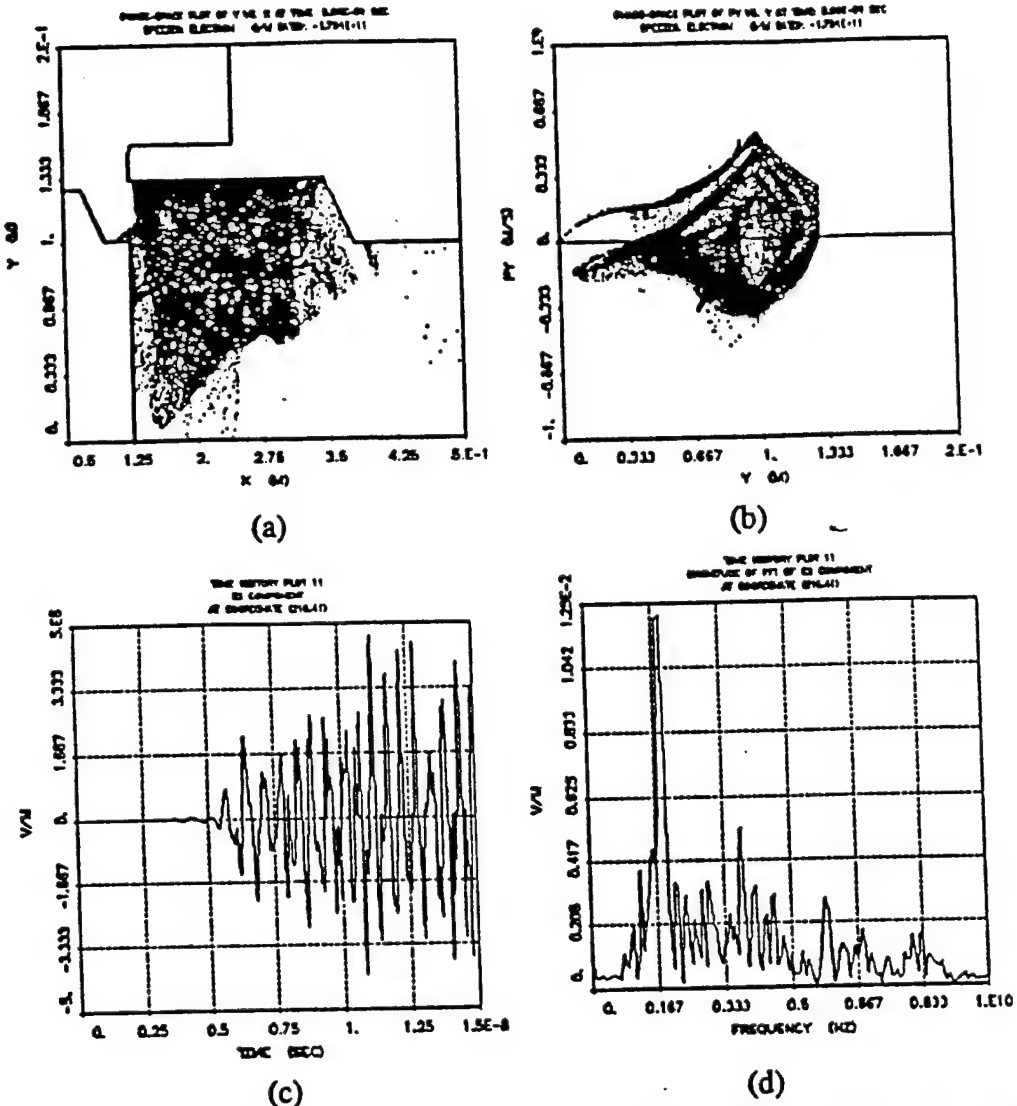

(a) (b) (c) (d)

Figure 5: Simulation results for Model A. (a) particle position at 2.5 ns, (b) r versus ρ_r at 2.5 ns, (c) E_r at wall versus time, (d) E_r at wall versus frequency.

Table 3: Simulation values for Model A geometry.

Parameter	Value
$r_a=r_{wz}$	98.4 mm
r_k	131.7 mm
l_a	186.5 mm
l_k	208.7 mm
transition	45° angle
l_{at}	35.5 mm
l_{kt}	6.7 mm

Parameter	Value
Diode Voltage (V_d)	500 kV
Diode Current (I_d)	55 kA
Diode Impedance (Z_d)	9.1 Ω
Beam Power (P_{beam})	27.5 GW
Microwave Frequency (f)	1.7 GHz
Microwave Power (P_{mw})	49.5 MW
Power Efficiency (η)	0.18%

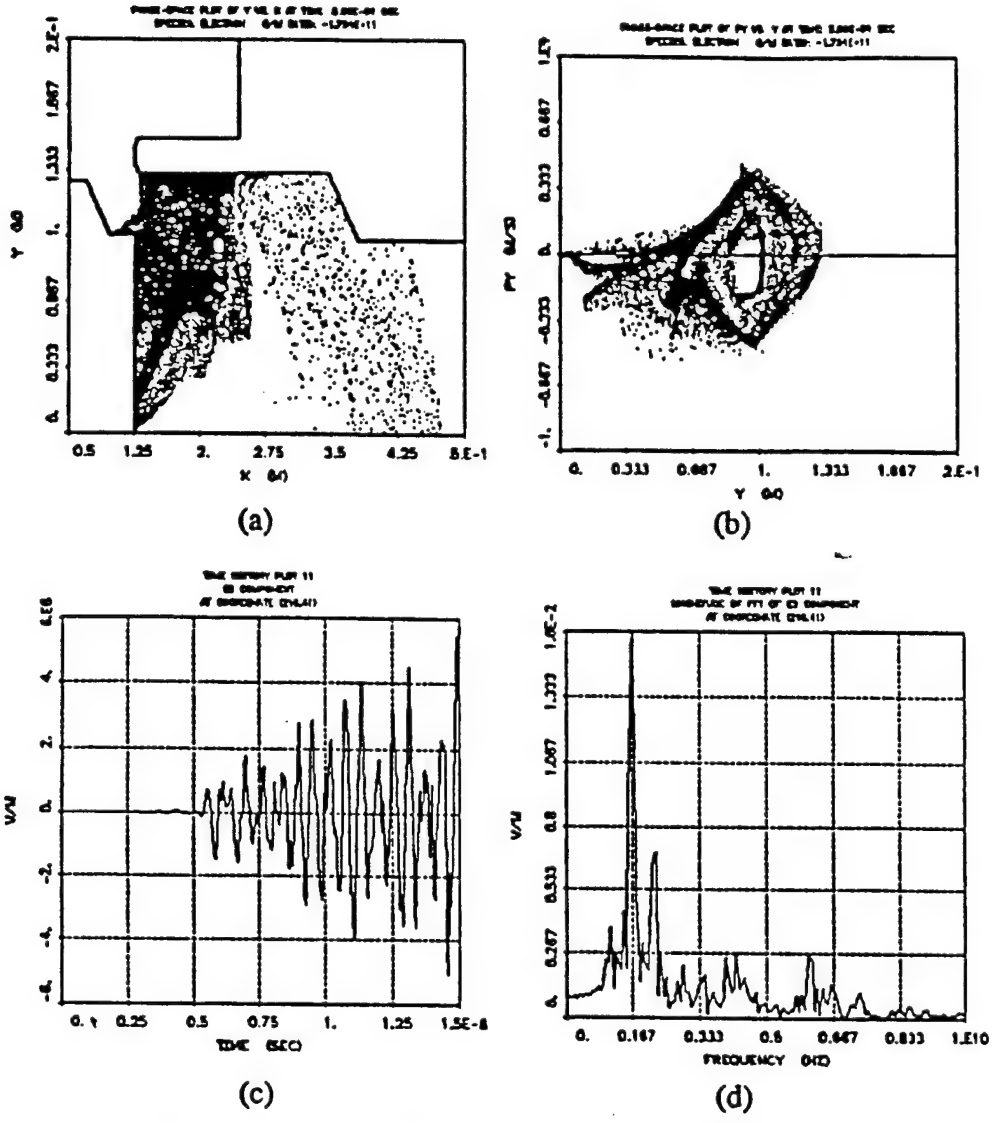

Figure 6: Simulation results for Model B. (a) particle position at 2.5 ns, (b) r versus ρ_r at 2.5 ns, (c) E_r at wall versus time, (d) E_r at wall versus frequency.

Table 4: Simulation values for Model B geometry.

Parameter	Value
$r_a=r_{wg}$	98.4 mm
r_k	131.7 mm
l_a	93.2 mm
l_k	208.7 mm
transition	45° angle
l_{a1}	128.8 mm
l_{k1}	6.7 mm

Parameter	Value
Diode Voltage (V_d)	520 kV
Diode Current (I_d)	45 kA
Diode Impedance (Z_d)	11.6 Ω
Beam Power (P_{beam})	23.4 GW
Microwave Frequency (f)	1.67 GHz
Microwave Power (P_{mw})	87 MW
Power Efficiency (η)	0.37%

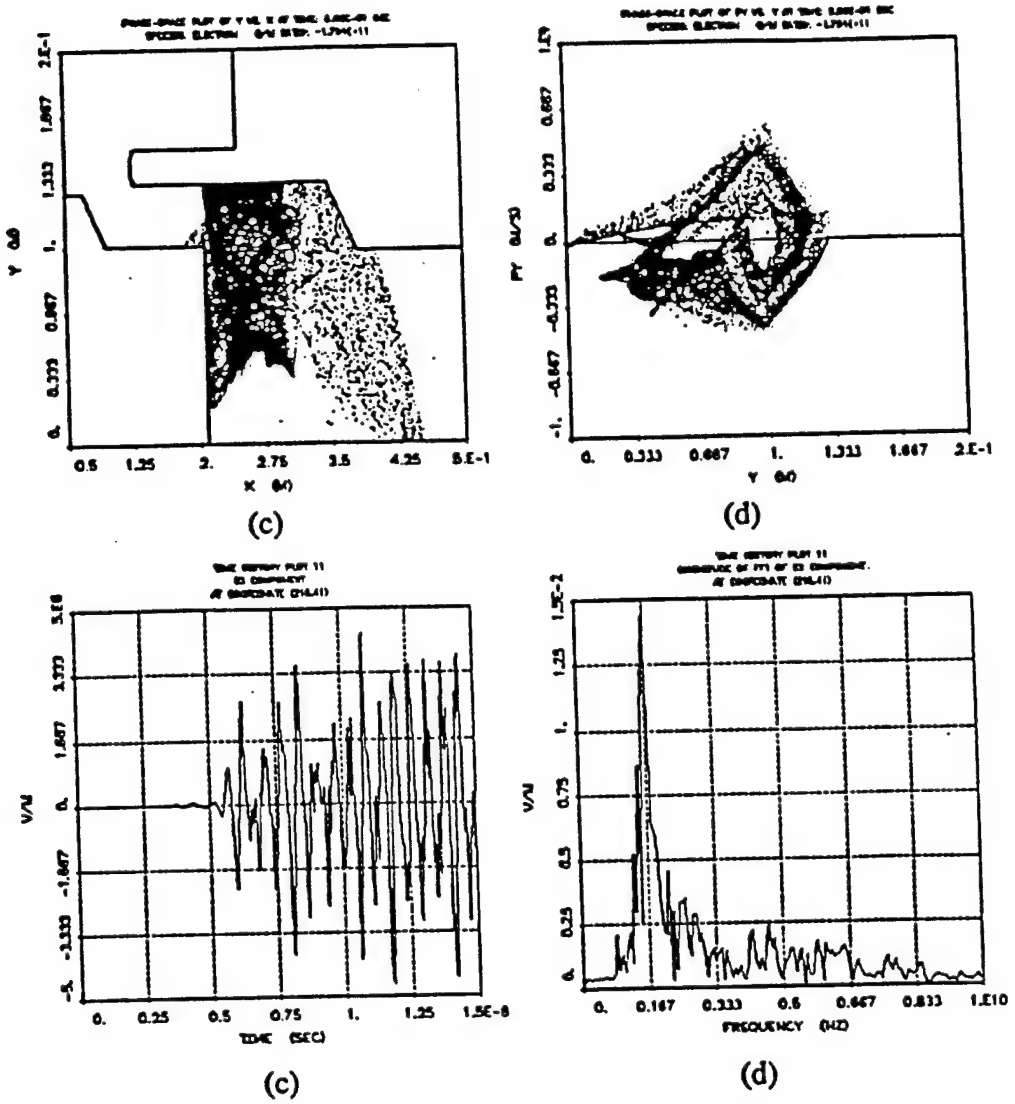

Figure 7: Simulation results for Model C. (a) particle position at 2.5 ns, (b) r versus ρ_r at 2.5 ns, (c) E_r at wall versus time, (d) E_r at wall versus frequency.

Table 5: Simulation values for Model C geometry.

Parameter	Value
$r_a=r_{wg}$	98.4 mm
r_k	131.7 mm
l_a	93.2 mm
l_k	93.2 mm
transition	45° angle
l_{at}	44.4 mm
l_{kt}	44.4 mm

Parameter	Value
Diode Voltage (V_d)	570 kV
Diode Current (I_d)	42 kA
Diode Impedance (Z_d)	13.6 Ω
Beam Power (P_{beam})	23.9 GW
Microwave Frequency (f)	1.67 GHz
Microwave Power (P_{mw})	78.6 MW
Power Efficiency (η)	0.32%

showed that power was being transmitted on axis. This was unexpected because a TM_{01} mode was expected for the symmetric source and modes with a transverse electric component on axis are asymmetric. Pictures of the radiation patterns were taken with the use of neon bulbs in the far field and only the TE_{11} mode radiates a pattern on axis in the far field indicating a TE_{11} mode was being produced. It was eventually discovered that the gap between the anode and the cathode was skewed which probably caused a larger bunching of electrons where the gap was smaller and a smaller bunching of electrons where the gap was larger. A re-alignment of the gap was performed but still resulted in the asymmetric mode. This asymmetric mode was probably caused by plasma instabilities and indicates that gap alignment is a sensitive parameter to the mode produced. Thus, a TE_{11} was being propagated and since a symmetric mode was originally expected from a symmetric source, only one probe was initially installed and a second E-field probe was, therefore, added for the measurement of total microwave power.

With the increased diagnostics, a test of the variable parameters was performed and is shown in Table 6. The test results were obtained by taking five similar shots for each configuration and averaging the results. The parameters in the table are defined as follows:

l_a = anode length

l_k = cathode length

l_{at} = distance between anode and transition

l_{kt} = distance between cathode and transition

V_{peak} = maximum diode voltage

I_{peak} = maximum diode current

Z_{diode} = diode impedance, V_{peak} / I_{peak}

P_{beam} = maximum microwave power

E_{beam} = energy in the electron beam

P_{mw} = maximum microwave power

E_{mw} = energy in the microwave pulse

η_{power} = power efficiency, $(P_{mw} / P_{beam}) \times 100\%$

η_{energy} = energy efficiency, $(E_{mw} / E_{beam}) \times 100\%$

Table 6: Complete listing of results for coaxial vircator tests.

Model	**A**	**A**	**B**	**B**	**C**	**C1**	**C2**	**C3**
Screen?	no	yes	no	yes	no	yes	yes	yes
l_a (mm)	187	187	93	93	93	93	93	93
l_k (mm)	207	207	207	207	210	210	120	93
l_{at} (mm)	36	36	130	130	45	45	45	45
l_{kt} (mm)	16	16	16	16	13	13	13	45
V_{peak} (kV)	629	533	672	620	696	646	629	616
I_{peak} (kA)	55.3	55.8	51.0	53.6	60.7	62.0	52.5	53.8
Z_{diode} (Ω)	10.8	9.5	13.2	11.5	11.4	10.4	11.9	11.4
P_{beam} (GW)	33.6	29.7	17.1	33.3	41.8	40.0	33.1	33.1
E_{beam} (J)	611	594	352	599	825	873	587	693
P_{mw} (MW)	87.5	105	4.7	153	16.9	173	176	218
E_{mw} (J)	3.46	4.55	0.15	6.45	0.62	6.62	8.39	11.9
η_{power} (%)	0.26	0.35	0.02	0.45	0.04	0.43	0.53	0.65
η_{energy} (%)	0.56	0.76	0.04	1.07	0.07	0.75	1.42	1.72
Frequency (GHz)	~1.4	~1.4	--	~1.9	--	~1.8	~1.9	~1.9

The average diode voltage and current waveforms for the tested geometries are shown in Figure 8 and the beam and microwave power waveforms are shown in Figure 9.

It is useful to note that the diode voltage always starts at around 38 ns and is on for around 25 ns when it drops to a lower value for another 25 ns while geometries that

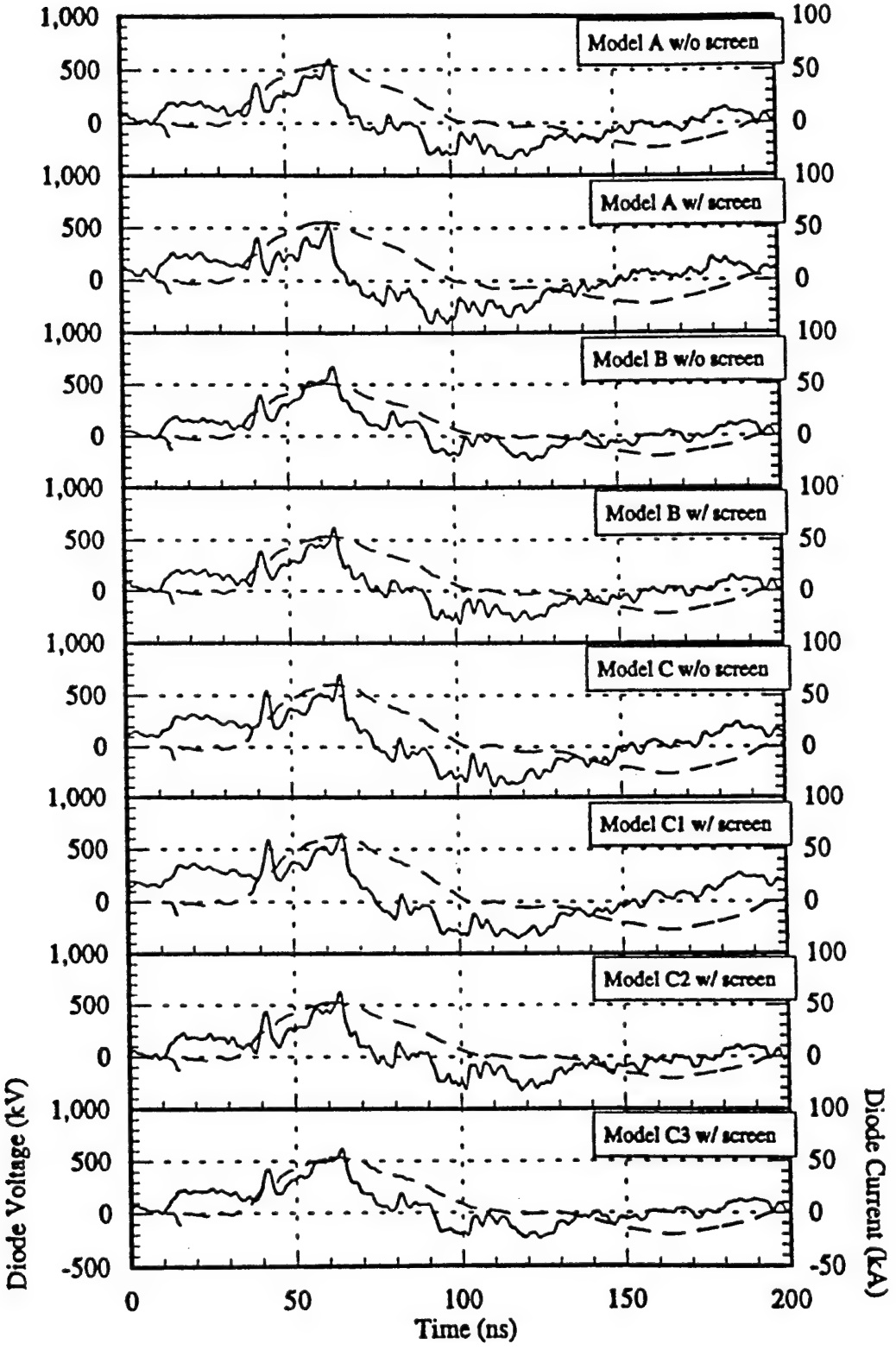

Figure 8: Average diode voltage (solid line) and current (dashed line) for the tested coaxial vircator geometries.

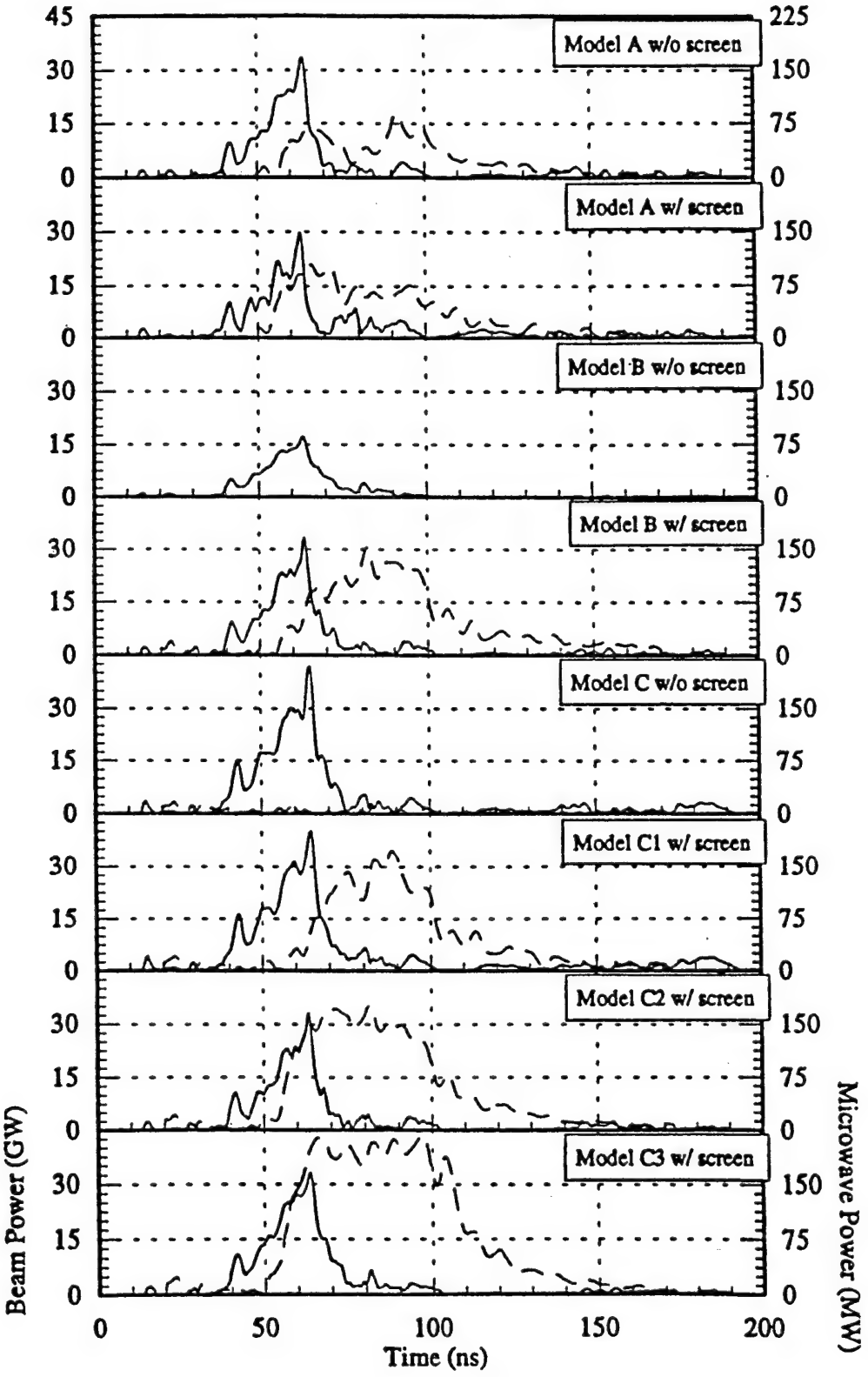

Figure 9: Average electron beam power (solid line) and microwave power (dashed line) for all the tested geometries.

had measurable microwave powers had microwave pulsed widths around 50 ns, not including the exponential decay.

In interpreting the results, it should be noted that the method for calculating the power efficiency is very conservative. The given values are minimums and should be considered lower limits. From the results, it is shown that microwave production is best in the geometries with the shorter anode structure, but only when wrapped with the screen. However, in Model A where the anode is longer, microwaves are produced whether or not the screen is present.

For the virtual cathode to oscillate within the anode cylinder, two things must occur. The virtual cathode must form, caused by the bunching of electrons exceeding the space charge limit, and a mechanism must exist for some dissipation of electrons. Otherwise, if the electrons are permanently trapped, all new incoming electrons will be deflected and the virtual cathode will never drop below the space charge limit and no oscillations will occur.

For the short anode, a mechanism for sufficient electron dissipation can be better realized than for the long anode structure. Electrons can be collected on the end plate or squirted out the end. For the longer anode a larger fraction of electrons occupy the area inside the ends of the anode structure, leading to a smaller rate of electron dissipation. This effect can be seen in the phase space plots from the MAGIC simulations in Figures 5 to 7. At the edges of the anode, the virtual cathode extends closer to the center due to the dissipation mechanism.

Information about coaxial vircator operation can also be obtained from variations of the geometries with and without the screen. For the virtual cathode to form, the

electrons must lose all of their kinetic energy to the potential energy of the virtual cathode. Without the screen, regularly spaced rods create an azimuthal electric field which deflects the incoming electrons. Then, incoming electrons slow down inside the anode cylinder, they lose the radial component of velocity but not the azimuthal component. The electrons turn away and do not form a virtual cathode. Thus, the virtual cathode that forms is less dense.

Based on these ideas, it is apparent that for efficient microwave generation, a coaxial vircator must impart a uniform, radial velocity to the electrons in the anode-cathode gap and that a short anode structure improves the dissipation mechanism for the virtual cathode which in turn increases the microwave production substantially.

A comparison of simulation and experiment shows a close correlation. This is remarkable due to the fact that power diagnostics for the simulation were on the assumed TM_{01} mode and experiment showed a TE_{11} mode present and is the basis for the experimental diagnostic calculations.

Another major effect seen from the experimental testing was a microwave pulse which was long compared to the beam power pulse which was the cause for a larger energy efficiency compared to power efficiency. Earlier experiments on a planar vircator did not show this effect. This is because virtual cathode formation in the planar vircator can only be sustained by continual injection of electrons. The coaxial vircator, on the other hand, creates a microwave pulse beyond the applied pulse. A possible explanation for this may lie in the cylindrical bunching of electrons. When the first high voltage pulse enters the diode, the velvet lining of the cathode becomes an explosive emitter and a plasma forms and acts as a source for electrons. After the initial pulse, reflections

inherent in the system leave a substantially lower voltage across the diode. This lower voltage level, though not large enough to initially form the virtual cathode, is high enough to accelerate the electrons across the gap and sustain the virtual cathode.

Efficiency Improvements

It is believed that the efficiency of the coaxial geometry is dependent upon a phenomena known as electron phase separation[5]. Phase separation refers to what are termed wrong-phased electrons and right-phased electrons. The wrong-phased electrons are the electrons that are accelerated at the expense of energy from the microwave field. The right-phased electrons are the electrons that are trapped in the potential well between the real and virtual cathodes. In the coaxial geometry, the right-phased electrons oscillate in the potential well and the wrong-phased electrons move toward the center axis where they are repelled by Coulombic forces. Thus, the wrong-phased electrons are caught in the interaction space, stored there, and radiate their own microwaves out of phase with the right-phased electrons.

Among the things that can be done to increase the efficiency, the most important is to eliminate competition between the various mechanisms that produce microwaves. This can be done by matching the reflexing and plasma frequencies, or eliminating one source of microwave production to let the other dominate, as in the reditron. The geometry under consideration is different from the planar geometry in terms of how it reacts to the microwaves produced. In a typical planar geometry, microwave production is based only on the current density due to the lack of a cavity and it is this feature that gives it its tunability. On the other hand, the coaxial geometry has a diode impedance of about ten ohms and a propagating wave impedance which is much larger, creating a

condition like a cavity. In actual experiments, the frequencies radiating the strongest are approximately the resonant frequencies of the cavity produced by the anode screen.

The experiments performed were aimed at increasing the efficiency by keeping electrons out of the wrong-phased region. Placing a conducting rod down the center of the geometry draws more electrons into the wrong-phased region, decreasing the efficiency, while the placement of a hole on the center had the opposite effect. To further increase the efficiency, simulations were performed with an annulus, at varying radii in the anode base, to better match the fields in the interaction region. Finally, for the given geometry, the interaction region, in the absence of electrons, has a constant static field. Pulsing the geometry, with an opposite polarity would give the electrons in the wrong-phased region an acceleration out of the interaction region, which would increase the efficiency.

Finally, the nature of the coaxial vircator allows the virtual cathode to be formed easily. The electrons continually accelerate inward with a decreasing volume and eventually the space-charge limiting current will be reached. This could also be an important factor in achieving a higher efficiency. Since the frequency of oscillation is only loosely related to applied voltage, decreasing it would have little effect on the virtual cathode formation but could significantly increase the efficiency.

Simulations

Due to the complex and highly unstable nature of the interactions in the vircator, simulations are needed to gain any insight into the behavior of the device. MAGIC and SOS, $2\text{-}^1/_2$ and 3 dimensional particle-in-cell codes, were used to simulate the various geometries. Figure 10 shows the simulated geometry.

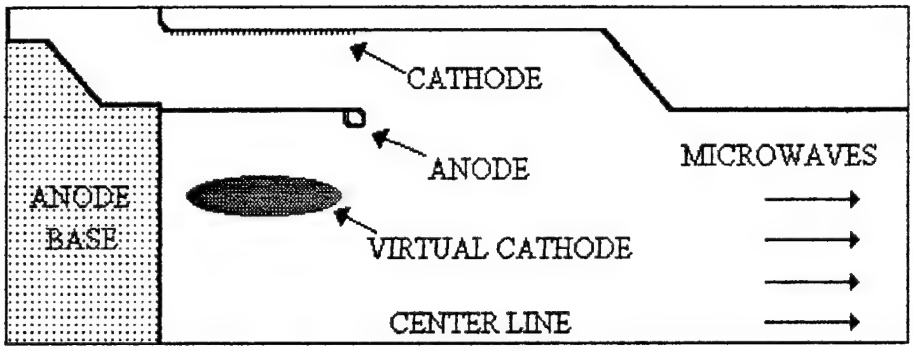

Figure 10: Simulated Coaxial Vircator Geometry

Initially, it was thought that placing a center conducting rod down the center of the device would increase the efficiency by collecting the electrons in the wrong-phase region. MAGIC simulations were run to determine the effectiveness of a rod and was found to increase the bandwidth but decrease the radiated amplitude at any one frequency. The cause was the rod pulling more electrons into the wrong-phased region, but the electrons were getting collected and not allowed to oscillate and destructively interfere with the radiation produced by the right-phased electrons. Generally, a coherent signal is desired and this produced the opposite effect. Yet, it did show the impact that the wrong-phased electrons have.

To create a coherent signal with a larger amplitude, electrons must be kept out of the wrong-phased region. Simulations were run with a hole placed in the center of the anode base to create an impedance mismatch that would create a field that would keep electrons in the right-phased region. Figure 11 shows the efficiencies of the different geometries at the dominant frequency normalized to the geometry with no rod or hole. Figure 12 shows the efficiencies of the different geometries taking total power into account, again normalized to the no rod or hole case. Since matching of the diode impedance to the transmission line impedance is important for maximum output power,

the diode impedance was calculated and found to be approximately the same in the different geometries, which indicates that the cause of the increase in efficiency is due to changes in the fields in the diode.

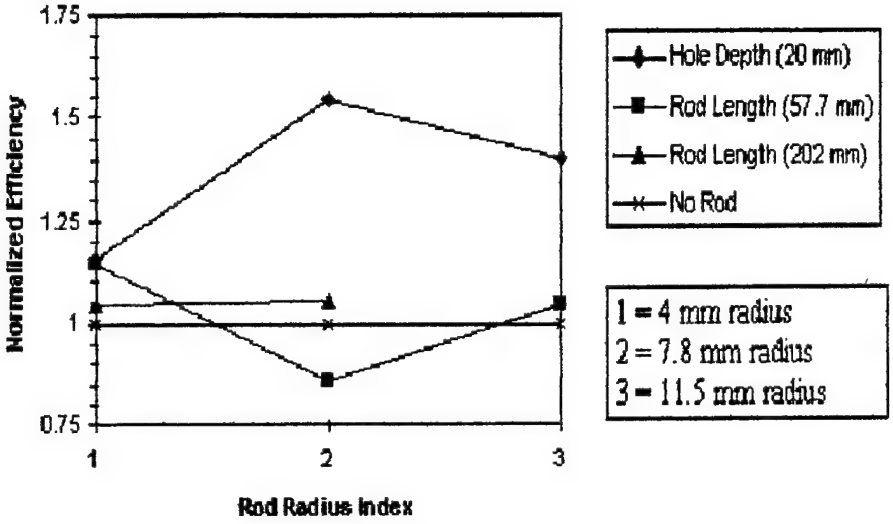

Figure 11: Efficiency at the Main Frequency Normalized to no Rod or Hole

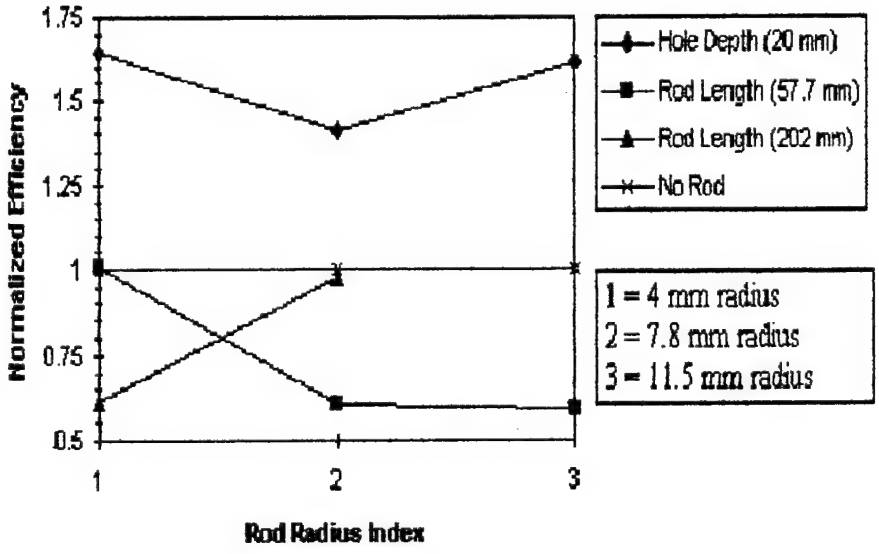

Figure 12: Efficiency Using Total Power Normalized to no Rod or Hole

It was thought that an annulus cut into the anode base at the appropriate radius, instead of a hole on center, might match the reflexing mechanism better. Figure 13 shows the geometry of the simulations performed. The variable "ra" is the distance from the centerline to the inner diameter of the annulus and "rh" is the width of the annulus. Figures 14 and 15 show the efficiency at the dominant frequency of the various parameters normalized to the no rod or hole case. The annulus depth is 2 cm. In the figures, the indexes on the horizontal axis represent the distance from the centerline to the start of the annulus. The index distances are: 1 corresponding to 3.18 cm, 2 corresponding to 3.85 cm, 3 corresponding to 4.51 cm, 4 corresponding to 5.18 cm, 5 corresponding to 5.85 cm, 6 corresponding to 6.51 cm, 7 corresponding to 7.18 cm, 8 corresponding to 7.84 cm, and 9 corresponding to 8.51 cm.

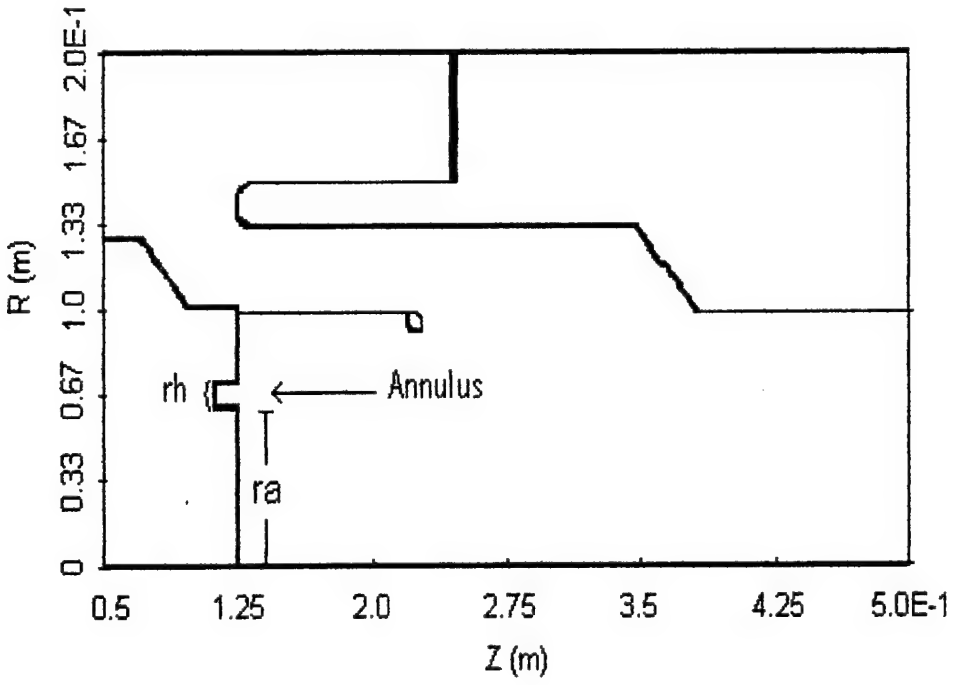

Figure 13: Coaxial Vircator with annulus.

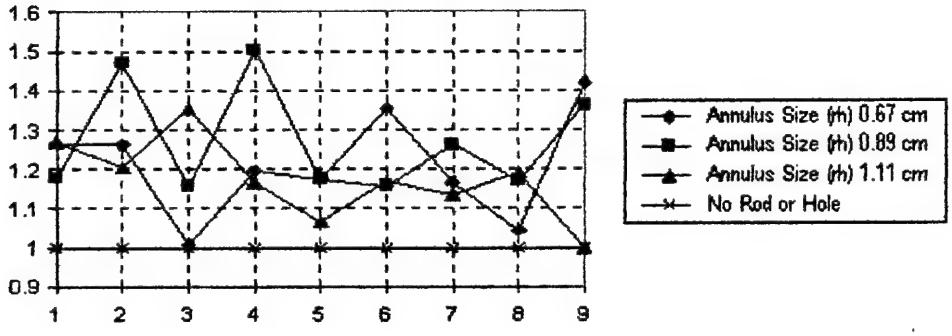

Figure 14: Efficiency with an Annulus at the Main Frequency Normalized to no Rod or Hole

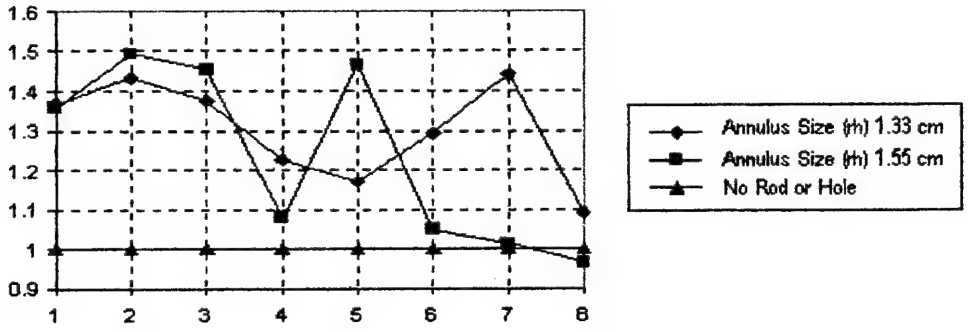

Figure 15: Efficiency with an Annulus at the Main Frequency Normalized to no Rod or Hole

Figures 16 and 17 show the efficiency of the overall power of the various parameters normalized to the no hole or no rod case.

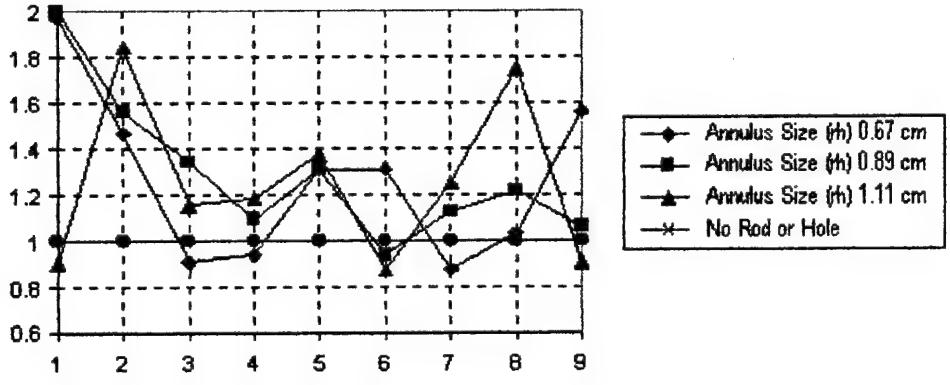

Figure 16: Efficiency with an Annulus Using Total Power Normalized to no Rod or Hole

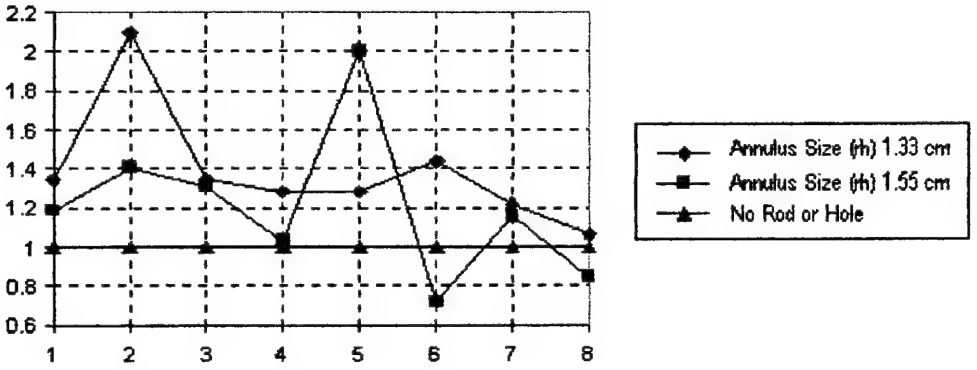

Figure 17: Efficiency with an Annulus Using Total Power Normalized to no Rod or Hole

All of the previous geometries were configured with the inner conductor, the anode base, pulsed positively and the outer conductor grounded. A geometry was tested where the inner conductor was pulsed negatively. This was designed to be implemented in the current system with little modification and is shown below in Figure 18.

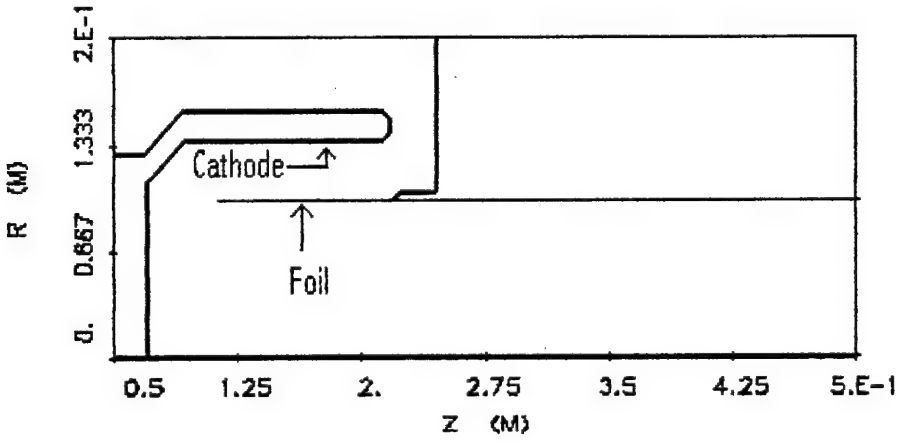

Figure 18: Negatively pulsed simulation geometry

The a-k gap for the negatively pulsed system was modified until the dominant frequency was comparable to the positively pulsed system frequency. The original system had an a-k gap of 3.11 cm and the negatively pulsed system had an a-k gap of 3.77 cm. Even with the dominant frequency of the negatively pulsed system matching

that of the positively pulsed system, it was still not set to maximize the output power since the transmission line impedance into the diode did not match the diode impedance. Yet, the efficiency still increased. The ratio of the normalized efficiency at the dominant frequency for the negatively pulsed system was found to be 1.91 times that of the positively pulsed system. The total normalized output power efficiency of the negatively pulsed system to that of the positively pulsed system was found to be 1.34.

It was found that bunches of electrons are transmitted down the waveguide. For the negatively pulsed system, these transmitted electrons were significantly larger in number than those in the positively pulsed system where the electrons are drawn towards the positive potential. Hence, a natural mechanism existed to get rid of electrons in the virtual cathode region, allowing new electrons to enter into the region and give up their energy to the microwave field. Figure 19 shows the phase-space plots for the two systems. From the plots, the number of electrons in the wrong-phased region and the strength of virtual cathode formation can be seen. Also, the kinetic energy of the beam can be calculated from the phase-space plots. Figure 20 shows the FFT for these systems.

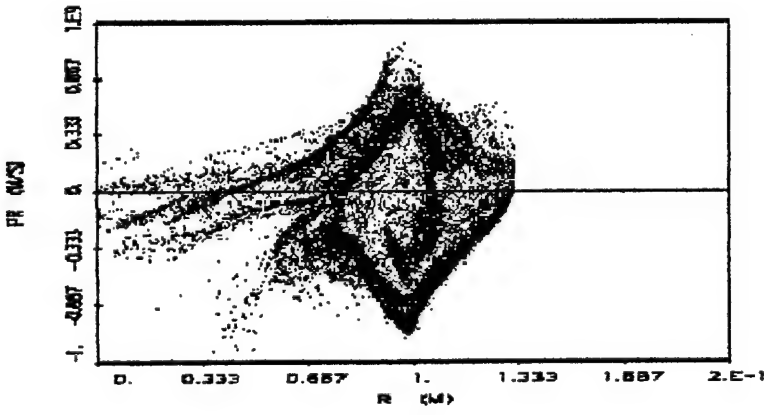

Figure 19A: Phase-space Plot for the Positively Pulsed System

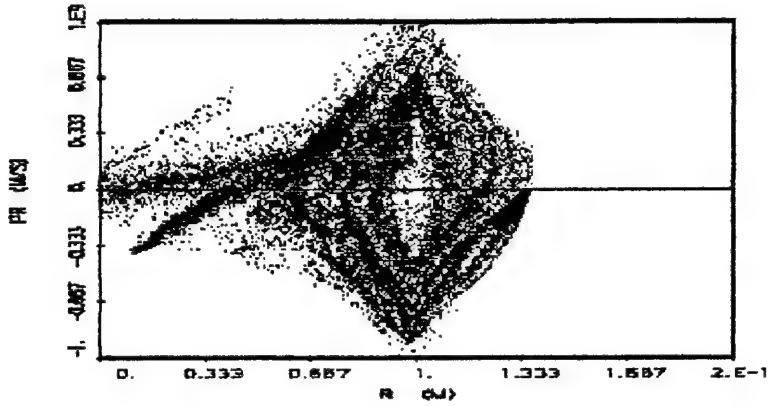

Figure 19B: Phase-space Plot for the Negatively Pulsed System

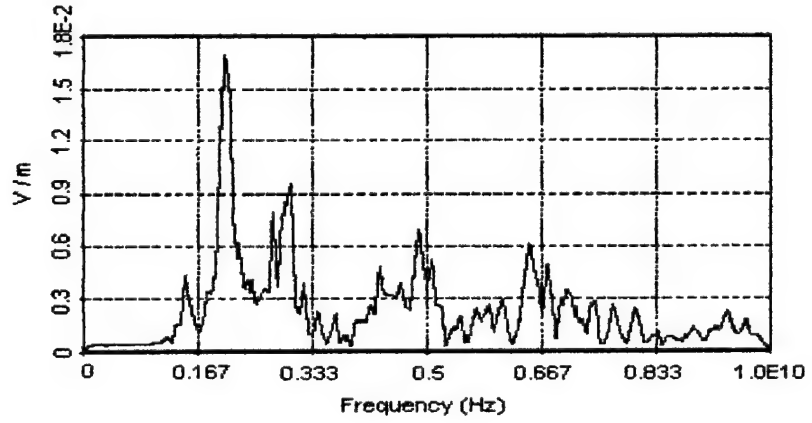

Figure 20A: FFT for the Positively Pulsed System

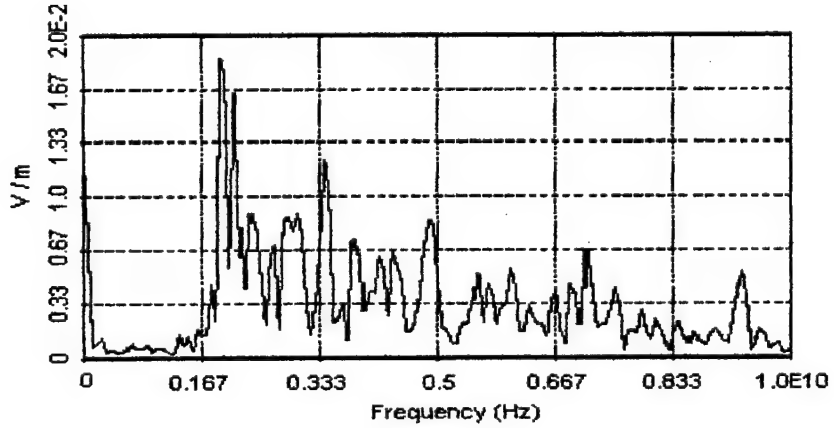

Figure 20B: FFT for the Negatively Pulsed System

Voltage Experiments

The final test for efficiency improvement was to match the plasma and reflexing frequencies. This was achieved by decreasing the applied voltage across the anode-cathode gap. Since the plasma frequency is related to the applied voltage in the following way:

$$f_{plasma} \sim V^{1/2}$$

and the reflexing frequency in the following way:

$$f_{reflex} \sim V^{3/2}$$

the voltage can be adjusted until the two correspond. Figures 21 and 22 show the diode powers and corresponding E-field probe outputs respectively for the high and low voltage shots. Figures 23 and 24 show typical rf waveforms and the corresponding FFT's from the E-field probes.

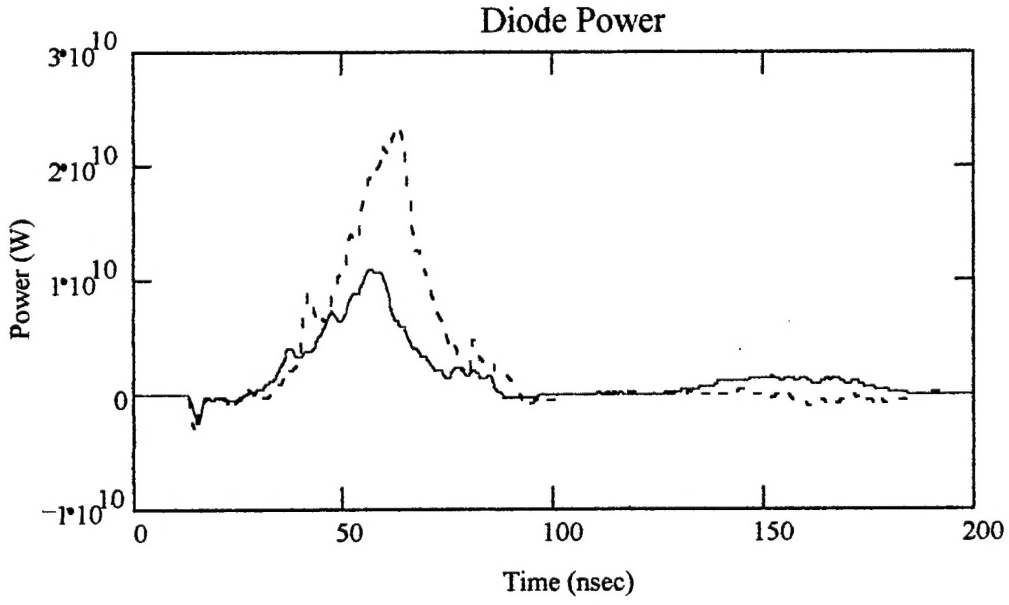

Figure 21: Diode Power. (Dashed line – high voltage)
(Solid line – low voltage)

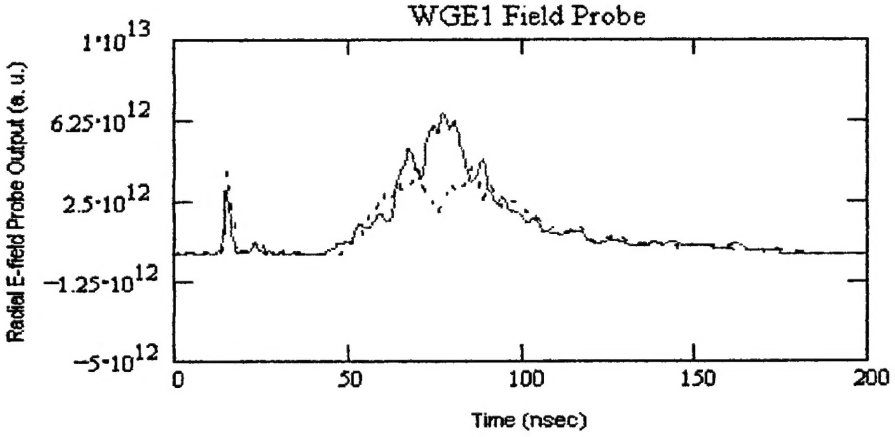

Figure 22A: E-field Probe Output. (Dashed line – high voltage)
(Solid line – low voltage)

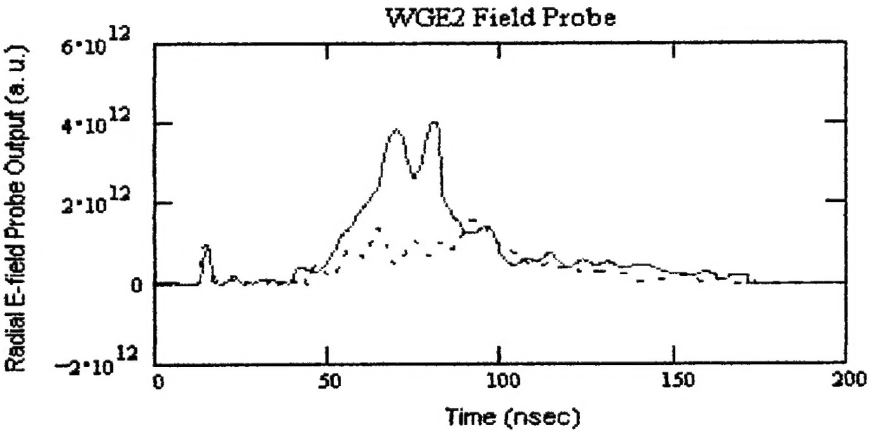

Figure 22B: E-field Probe Output. (Dashed line – high voltage)
(Solid line – low voltage)

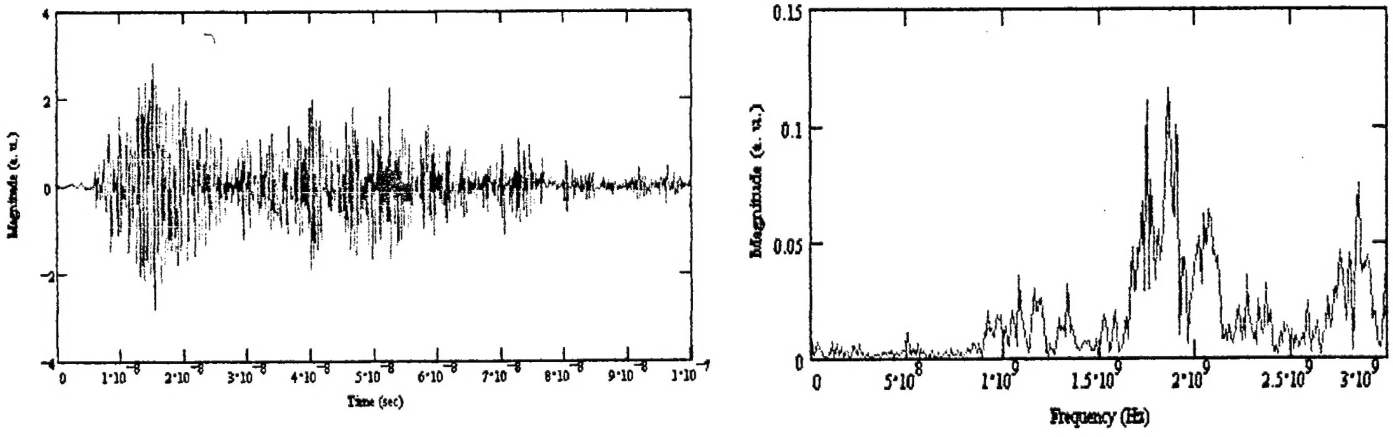

Figure 23: High Voltage rf waveform from E-field probe and FFT

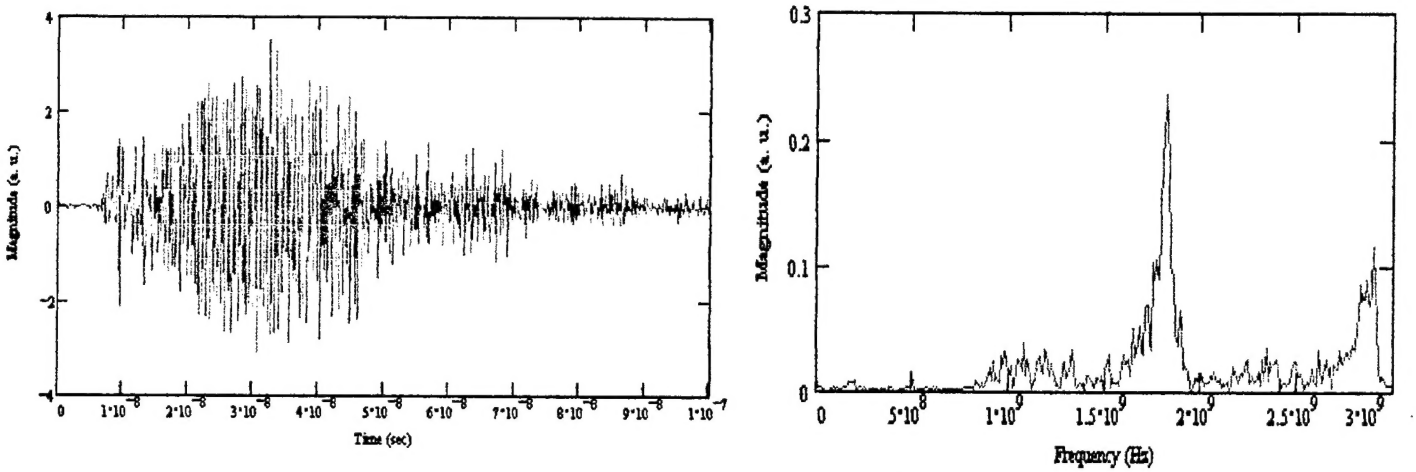

Figure 24: Low Voltage rf waveform from E-field probe and FFT

From the FFT of the high voltage experiment, two frequencies can be seen, one at 1.8 GHz and one at 2.1 GHz, which correspond to the plasma and reflexing frequencies. As the voltage is decreased, the 2.1 GHz frequency decreases until at a certain value, it corresponds to the 1.8 GHz signal. Furthermore, since the plasma frequency is only loosley related to the applied voltage, a small change in voltage will result in little change in the plasma frequency but a larger change in reflexing frequency. Hence, one can conclude that the 1.8 GHz frequency is due to the plasma oscillations and the 2.1 GHz signal is due to the reflexing electrons. It can be seen from the figures that a significant increase in output power can be achieved with a reduction in applied voltage by matching the two frequency components.

Conclusion

The purpose of this study was to investigate the viablility of a coaxial vircator and test geometries that increase the vircator efficiency. It was found that the coaxial vircator is a high-power microwave device comparable to the planar geometry. It was found that placing a rod down the center drew more electrons into the wrong-phased region,

decreasing the radiation at a given frequency and increasing the overall bandwidth, but placing a hole in the center increased the efficiency by producing a field that kept more electrons in the right-phased region. Changing the hole in the center into an annulus increased the efficiency further. Changing the system from a positively pulsed system into a negatively pulsed system created a mechanism for electrons to be eliminated from the virtual cathode region. This also eliminated electrons in the wrong-phased region and significantly increased the efficiency. Finally, altering the applied voltage allowed the plasma and reflexing frequencies to be matched giving an increase in efficiency. Further improvements might be made by combining the effects, placing an annulus in a negatively pulsed system with an appropriately applied voltage.

---

1 Benford, J., Swegle, J., "High-Power Microwaves", Boston: Artech House, Inc. 1992.

2 S. B. Bludov, N. P. Gadetskii, K. A. Kravtsov, et. al., "Generation of High-Power Ultrashort Microwave Pulses and their Effect on Electronic Devices", Plasma Physics Reports, vol. 20, no.8, 1994, pp. 712-717.

3 V. P. Grigoryev, et al, "Experimental and Theoretical Investigations of Generations of Electromagnetic Emission in the Vircators," Proceedings of the 8th International Conference on High-Power Particle Beams, 1990, pp. 1211-1216.

4 Crawford, M.,Ph.D. Dissertation, Texas Tech University, 1994.

5 Selemir, V. D., Alekhin, B. V., et. al., Plasma Physics Reports, 1994, vol. 20, no. 8, pp. 621-639.